JOURNAL OF CATALYSIS 27, 222–231 (1972)

Investigations of Molecules Trapped in Microporous Alumina Aerogels

II. Pore Structure of Aluminas

P. A. CUTTING AND N. D. PARKYNS

Gas Council, London Research Station, Michael Road, London SW6 2AD

AND

K. S. W. SING

Brunel University, Kingston Lane, Uxbridge, Middlesex, England

Received October 15, 1971

The pore structure of alumina aerogels which were previously shown by infrared spectroscopic studies to trap various molecules during their preparation, has been examined by adsorption of nitrogen and carbon tetrachloride. The α_s-plots were constructed from the nitrogen adsorption data and showed that the aerogels were strongly microporous and that both the micropore volume and the external surface area diminished as the aerogels are heated from 200 to 900°C. The carbon tetrachloride α_s-plots showed that although the alcohol-prepared aerogels exhibited a steadily diminishing adsorption capacity as the temperature was raised, those of the ether-prepared aerogels exhibited an upward deviation showing that extra pores in the 20 Å region had been created.

A model, based on infrared, electron microscope and adsorption data, is proposed of a three-dimensional mesh of alumina needles with initially restricted pore openings which may in some circumstances open up on heating.

INTRODUCTION

In Part I of this series (*1*) we gave spectroscopic evidence for the trapping of ethanol, diethyl ether and carbon dioxide in the pores of alumina aerogels. The results led us to postulate a different narrow pore structure for aerogels prepared using ethanol compared to that of those using other organic liquids because of the unique ability of the former to trap carbon dioxide formed by oxidation of the alcohol on heating in air to above 500°C.

Among methods of analyzing adsorption isotherms to obtain information about pore structure, the so-called "*t*-plot" developed by De Boer and his co-workers is fairly well established (*2–4*) and examples of its use are given by Broekhoff and Linsen (*5*). Criticism of the *t*-values used has been made by Pierce (*6*) who stated that the earlier figures of Cranston and Inkley (*7*) gave more consistently linear *t*-plots for oxides. Brunauer, Skalny and Bodor (*8*) have commented on the dependence of the *t*-plot analysis on locating the monolayer point of the reference isotherm accurately. A new modification introduced by Sing (*9*) and called by him the α_s-method, overcomes these criticisms and enables the analysis of isotherms of other adsorbates than nitrogen to be successfully undertaken.

In this paper, we have used both the *t*- and the α_s-plots to reveal the detailed narrow pore structure of the aerogels under study.

Copyright © 1972 by Academic Press, Inc.
All rights of reproduction in any form reserved.

EXPERIMENTAL METHODS

Materials. The aerogels were all fully described in Ref. (*1*). Nitrogen (99.95% purity) was obtained from cylinders and freed from water by passing it through a liquid nitrogen trap before use. Carbon tetrachloride was of "Analar" quality and was distilled before use.

Adsorption isotherms. Adsorption isotherms were all obtained on a Cahn RG electrobalance. About 0.1 g of sample was required: the limit of sensitivity was between 10^{-6} and 10^{-7} g. Nitrogen adsorption measurements were carried out at −196°C; isotherms and α_s-plots were corrected (*10*) for the slightly higher temperature of the sample bucket compared to that of the liquid nitrogen bath; because of this the highest relative pressure was 0.9. Pressures were measured on a 15 psia Bell and Howell transducer (type 4-353-0003) to ±0.05 Torr.

Krypton adsorption measurements were also carried out at −196°C: the low pressures involved (<4 Torr) were measured on a 1 psia Bell and Howell transducer (4-353-0001) to ±0.005 Torr.

Carbon tetrachloride isotherms were determined at 0°C. Pressures (up to 50 Torr) were measured on the more sensitive transducer.

Samples were treated as described in Ref. (*1*), that is, they were heated in steps of 100°C from 200 to 900°C either *in vacuo* or in oxygen as appropriate. Electron micrographs were taken by Dr. F. E. Shephard of these laboratories using a JEM-7 instrument. Samples were made by embedding the aerogel in methacrylate polymer and cutting thin sections with a microtome. All micrographs were obtained by the transmission technique.

RESULTS

Preliminary studies. Two representative samples of ether- and alcohol-prepared aerogels were heated in air at 600°C for 6–8 hr. Nitrogen adsorption isotherms showed typical type II behavior. The BET surface area for the ether-prepared aerogel was 220 $m^2\,g^{-1}$ and for the alcohol-prepared aerogel, 145 $m^2\,g^{-1}$. Krypton adsorption (at −196°C) gave much lower BET surface areas, 128 and 83 $m^2\,g^{-1}$, respectively (assuming the molecular area to be 19.5 Å^2).

It was clear that there was a significant difference between the surface properties of the two types of aerogel, but the exact nature of this difference was not made clear by measuring the BET surface area only. Much more detailed information became available from adsorption isotherms determined on samples which were heated from 200 to 900°C in steps of 100°C.

Nitrogen adsorption isotherms. Three samples were chosen for intensive study, one prepared using ethanol, another using ether and a third using *n*-hexane [Batches II, III, and VIII, respectively, see Ref. (*1*)]. These were heated as described above, both in oxygen and *in vacuo*. All the nitrogen isotherms generally followed the reversible type II classification up to the highest pressures used ($p/p_0 = 0.9$); there was no sign of hysteresis.

From the isotherms, α_s-plots were constructed using the standard α_s data of Payne and Sing (*11*) for Degussa alumina "C". They are shown in Figs. 1 and 2. Values of external surface area were derived from the slope of the upper linear portion ($t > 7$ Å) and are shown in Table 1.

BET surface areas were also calculated from the conventional BET plot and are shown in Table 1 in parentheses.

The micropore volume is given by extrapolating the upper linear part of the α_s-plot to the V_a axis where the intercept represents the amount required to fill the micropores. This procedure, which is due to Sing (*12*), gives values recorded in Table 2.

Carbon tetrachloride isotherms. Carbon tetrachloride adsorption isotherms were near type III as the "knee" was generally rather ill-defined. The adsorption increased sharply as $p/p_0 \rightarrow 1.0$ making precise determination of the upper part of the isotherm difficult. Typical isotherms are shown in Fig. 3 together with the "standard isotherm" for alumina type C (*13*). Derived α_s-plots are shown in Fig. 4. Previous

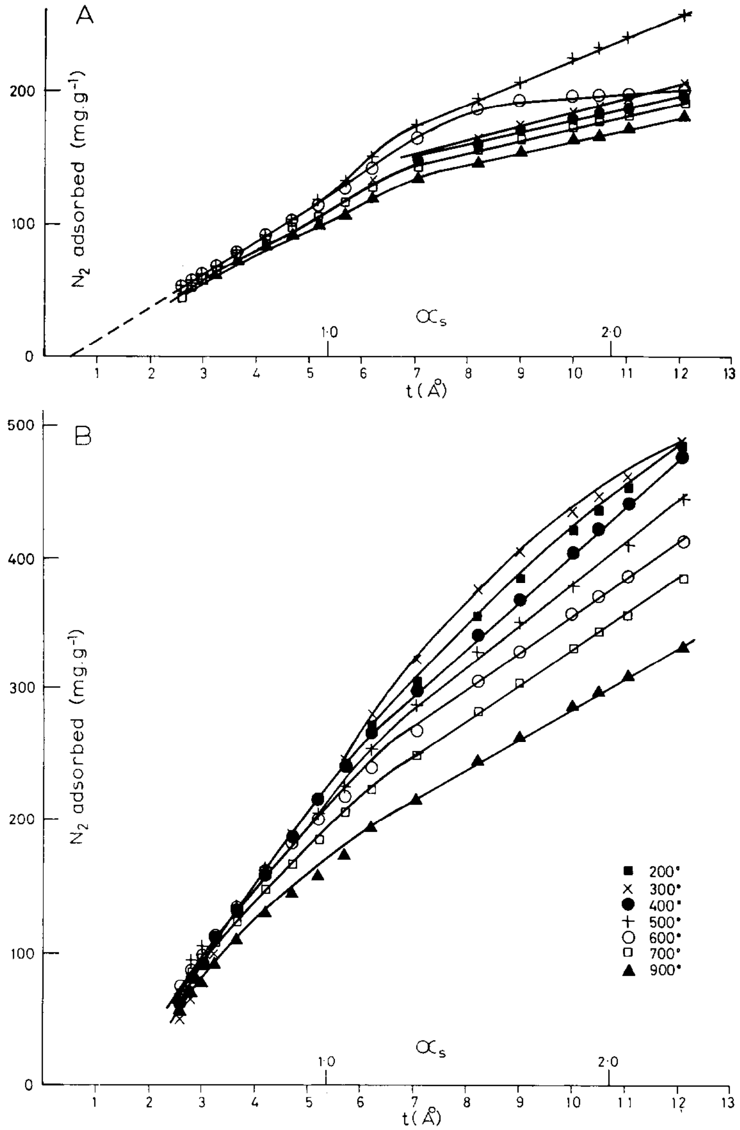

FIG. 1. Nitrogen α_s-plots for aerogels heated *in vacuo* to the temperatures shown. (A) Ethanol-prepared aerogel; (B) ether-prepared aerogel.

work had shown that the values of surface area obtained by applying the BET equation to carbon tetrachloride isotherms for various well-characterized adsorbents were either too low or too high, depending on the absence or presence of micropores (*13*). Accordingly, the BET method has not been employed to analyze the carbon tetrachloride isotherms.

Electron micrographs. Electron micrographs of alcohol- and ether-prepared aerogels heated to 600°C for 6 hr in air showed that both types were in the form of needles. These were on average about 300 Å long by 60 Å wide and 150 × 30 Å, respectively, for the two types of aerogel. Much larger lamellae (about 1000 × 500 Å) were also present in both cases. The needles were not discrete but had a tightly knit structure. The micrographs were generally similar to those described by Peri (*14*) for uncalcined aerogels.

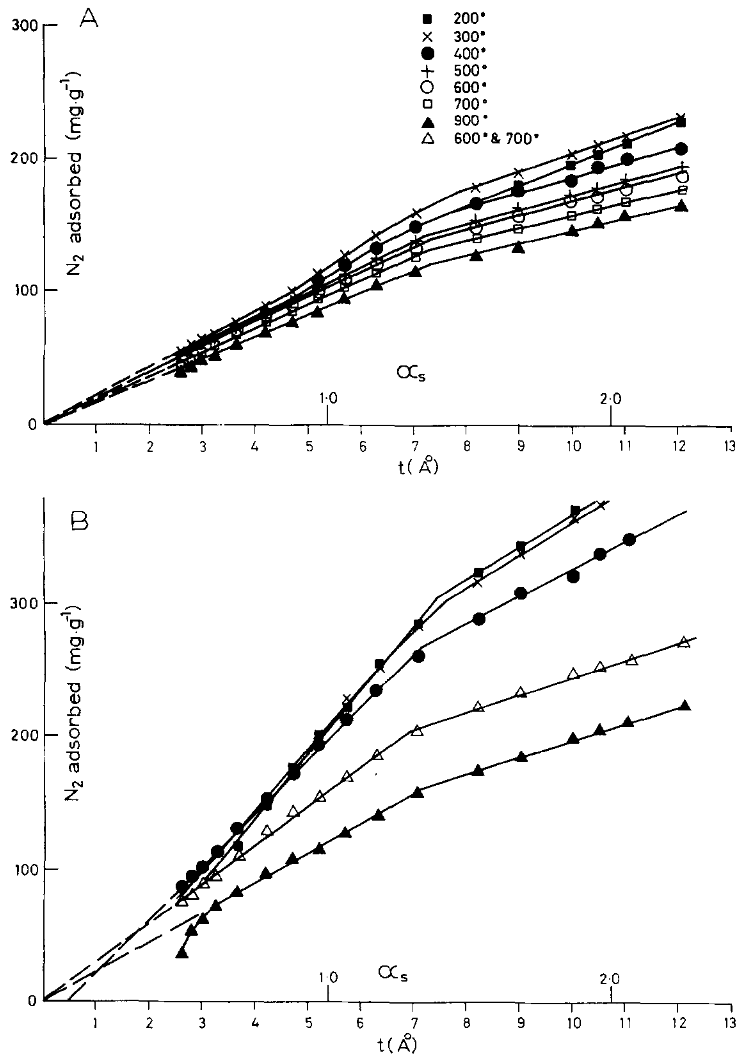

FIG. 2. Nitrogen α_s-plots for aerogels heated in oxygen to the temperatures shown. (A) Ethanol-prepared aerogel; (B) ether-prepared aerogel.

DISCUSSION

Sizes of molecules. In view of the ability of alumina aerogels to trap fairly simple molecules such as ethanol and carbon dioxide (*1*), it is clear that the physical size of molecules used as adsorbates in the adsorption isotherms is of the greatest importance. Unfortunately, there are no definitive values for these molecular dimensions available in the literature.

A value of 4.3 Å for the diameter of the nitrogen molecule proposed by Shull (*15*) is generally adopted. His value for oxygen, 4.2 Å, shows that oxygen may diffuse into pores which are available to nitrogen and *vice versa.* Two values for the diameter of the symmetric carbon tetrachloride molecule have been calculated. The higher, 6.8 Å, was calculated from A_m by Kiselev and Aristov (*16*) from the liquid density assuming close packing: a lower value of 6.4 Å was obtained from electron diffraction measurements in the gas phase (*18*). The agreement between the two values is surprisingly good.

Turning to molecules which infrared spectra show are trapped in the small pores

TABLE 1

EXTERNAL SURFACE AREAS (m^2 g^{-1}) CALCULATED FROM THE NITROGEN α_s-PLOTS FOR ALUMINA AEROGELS AFTER HEATING TO THE TEMPERATURES SHOWN[a]

		Calcination temp (°C)						
	Sample	200	300	400	500	600	700	900
Heated in vacuum	Alcohol-prepared	128	128	109	222	32	111	103
	(II)	(250)	(246)	(238)	(268)	(265)	(265)	(240)
	Ether-prepared	—	—	442	390	346	336	286
	(III)	(470)	(466)	(474)	(474)	(449)	(430)	(346)
	n-Hexane-prepared	257	257	257	257	279	247	240
	(VIII)	(370)	(378)	(376)	(409)	(412)	(408)	(374)
Heated in oxygen	Alcohol-prepared	198	170	148	133	128	119	114
	(II)	(240)	(262)	(250)	(232)	(235)	(215)	(195)
	Ether-prepared	304	274	250	—	168	168	158
	(III)	(460)	(450)	(440)	(420)	(360)	(348)	(280)

[a] BET surface areas shown in parentheses.

of the aerogels, carbon dioxide is somewhat dumbbell-shaped. The values quoted for the length vary between 4.63 Å, as determined by electron diffraction (*18*), to 5.40 or 5.72 Å from van der Waals radii (*19*). The variation in the latter value arises from different coordination numbers possible in the packing of solid carbon dioxide. Hexter and Goldfarb (*20*) in a spectroscopic study of a quinol–CO_2 clathrate adopted Powell's earlier value of 5.23 Å and this seems appropriate to the present circumstances. Ethanol and diethyl ether are much larger molecules with a lower degree of symmetry. The electron diffraction data (*18*) show that ethanol has maximum lengths of 6.00 Å in the *trans* and 5.44 in the *gauche*-configuration. Ether is somewhat bigger, the corresponding values being 8.05 and 7.95 Å.

Although the actual values may not be correct it may be noted that the sizes of molecules increase in the order: N_2, $O_2 < CO_2 < CCl_4 < C_2H_5OH < C_2H_5OC_2H_5$.

Pore structures of alumina aerogels. The nitrogen α_s-plots (Figs. 1 and 2, A and B) for both types of alumina aerogel have breaks at $t = 7$ Å, followed by the downward deviation characteristic of microporous materials. However, because the break occurs at so high a value of t, it is likely that the initial linearity is due to a "compensation effect" whereby reversible capillary compensation in the narrower mesopores offsets the tendency towards a lower slope as a result of micropore filling. In

TABLE 2

PORE VOLUMES (cm^3 g^{-1}) DERIVED FROM α_s-PLOTS ON ALUMINA AEROGELS

		Calcination temp (°C)						
Sample	Adsorbate	200	300	400	500	600	700	900
Ether-prepared (III)	N_2	—[a]	—[a]	0.150	—[a]	0.137	0.137	0.085
Alcohol-prepared (II)	N_2	—[a]	0.082	0.084	0.080	0.080	0.077	0.068
Alcohol-prepared (II)	CCl_4	—[a]	—[a]	—[b]	0.105	—[b]	—[b]	0.087

[a] Anomalous α_s-plot.

[b] Isotherm not determined.

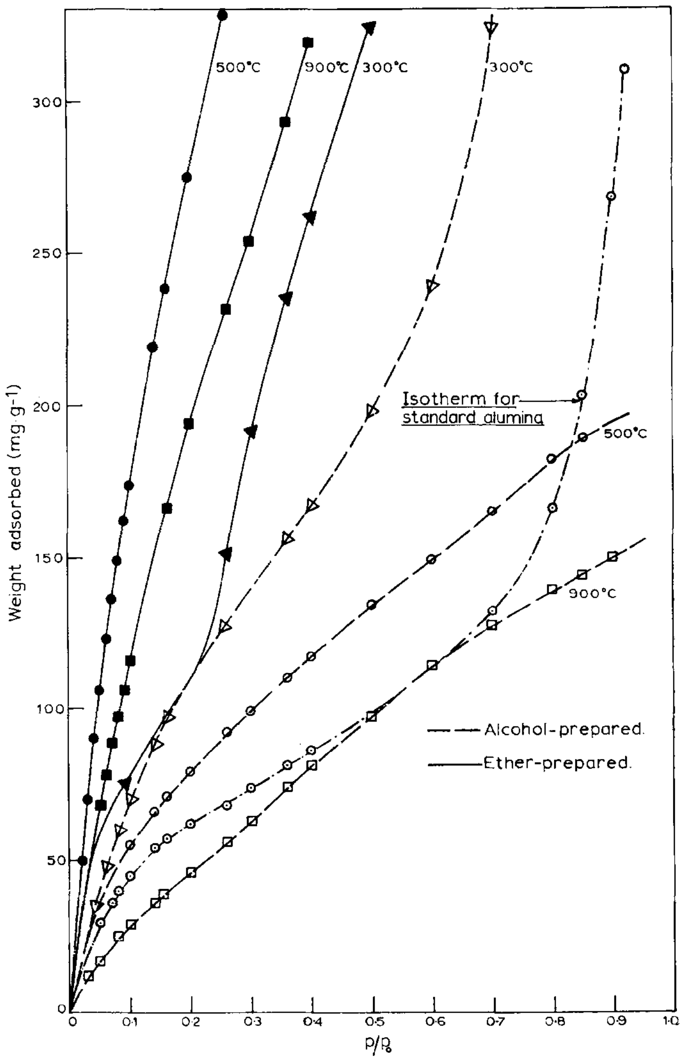

FIG. 3. Adsorption isotherms of carbon tetrachloride at 0°C on alumina aerogels heated to the temperature shown.

the case of a continuous distribution of pores between the micro- and the meso-region, this effect would not be unexpected.

Use of another adsorbate may overcome this problem and the more complex character of the carbon tetrachloride α_s-plots (Fig. 3) appears to confirm not only the microporous nature of the aerogels but also the existence of the compensation effect referred to above. The higher polarizability of carbon tetrachloride accentuates the effect of microporosity (*9*) and the larger physical size of the molecule also means that some of the narrower pores which behave as mesopores with respect to nitrogen act as micropores for carbon tetrachloride sorption.

There is a marked difference between the nitrogen α_s-plots for samples heated in vacuum (Fig. 1) and for those calcined in oxygen (Fig. 2). The former are much more irregular in their behavior and none of them passes through the origin on extrapolation, as do the majority of the latter. We ascribe this anomalous behavior to the deposition of carbonaceous material by

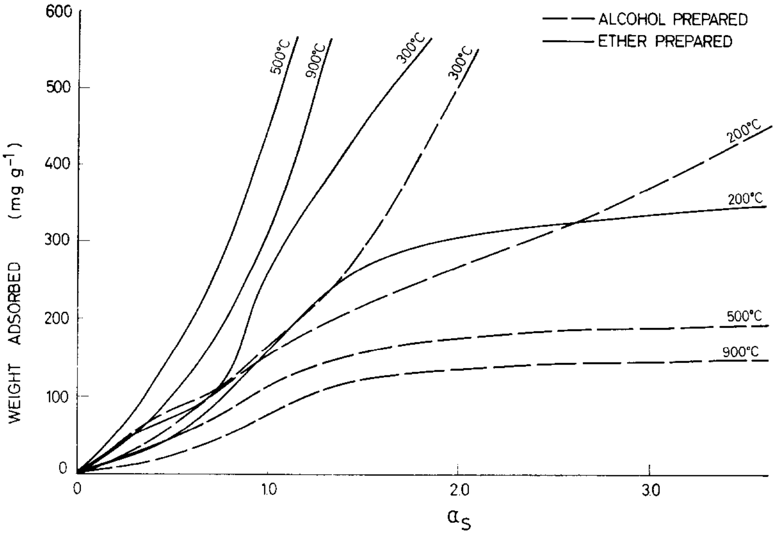

FIG. 4. Carbon tetrachloride α_s-plots for alumina aerogels heated in oxygen to temperatures shown. (– –) Alcohol-prepared aerogel; (—) ether-prepared aerogel.

pyrolysis of the trapped organic molecules; in the presence of oxygen this is converted to carbon dioxide, except at the lowest temperatures, giving an uncontaminated alumina surface. Failure of extrapolated t-plots or α_s-plots (in the low p/p_0 range) to pass through the origin is associated with the difference in c-values compared to those for the standard t-curve (*5*, *21*, *22*). In effect, we have produced a nonstandard surface by covering it with carbon and as a result, comparison with the standard alumina surface is no longer strictly correct. This effect disappears at higher relative pressures where multilayer adsorption of nitrogen is occurring and the additional adsorbed layers form on top of other nitrogen molecules without direct contact with the surface. Examples are seen in the results of Carruthers *et al.* (*22*) and Broekhoff and Linsen (*5*).

Effect of temperature on pore structure. The nitrogen α_s-plots show a progressive reduction in the uptake of gas with increase in the temperature of pretreatment of the aerogel. This is caused partially by a reduction in the micropore volume and more especially by a reduction in external surface area. Figure 5 shows how the latter declines steadily due to sintering as the temperature is increased. By comparison, the values for a hexane-prepared aerogel (sample VIII) remain remarkably constant.

The BET values given in Table 1 do not change in an exactly parallel way to the external areas, although they do tend to fall with increasing temperature as shown by the curve for ether-prepared aerogels given in Fig. 5. In the one case where a sufficient number of reliable values of micropore volume (strictly speaking, narrow pore volumes) could be calculated (see Table 2), i.e., for the alcohol-prepared aerogel heated in oxygen, they are found to run parallel to the corresponding BET values (in Table 1) in a remarkable way. This is to be expected, in view of the fact that any micropore filling contribution is located in the pressure region where BET plots are derived; this underlines the lack of meaning to be attached to BET areas for microporous solids.

The overall picture given by the nitrogen α_s-plots is of a gradual sintering for both alcohol- and ether-prepared aerogels, resulting in a continuous loss of external surface area and a proportionally smaller loss of narrow pore volume. However, there is apparently no radical difference in behavior between the two types of aerogel.

The position is quite different when we consider the carbon tetrachloride α_s-plots.

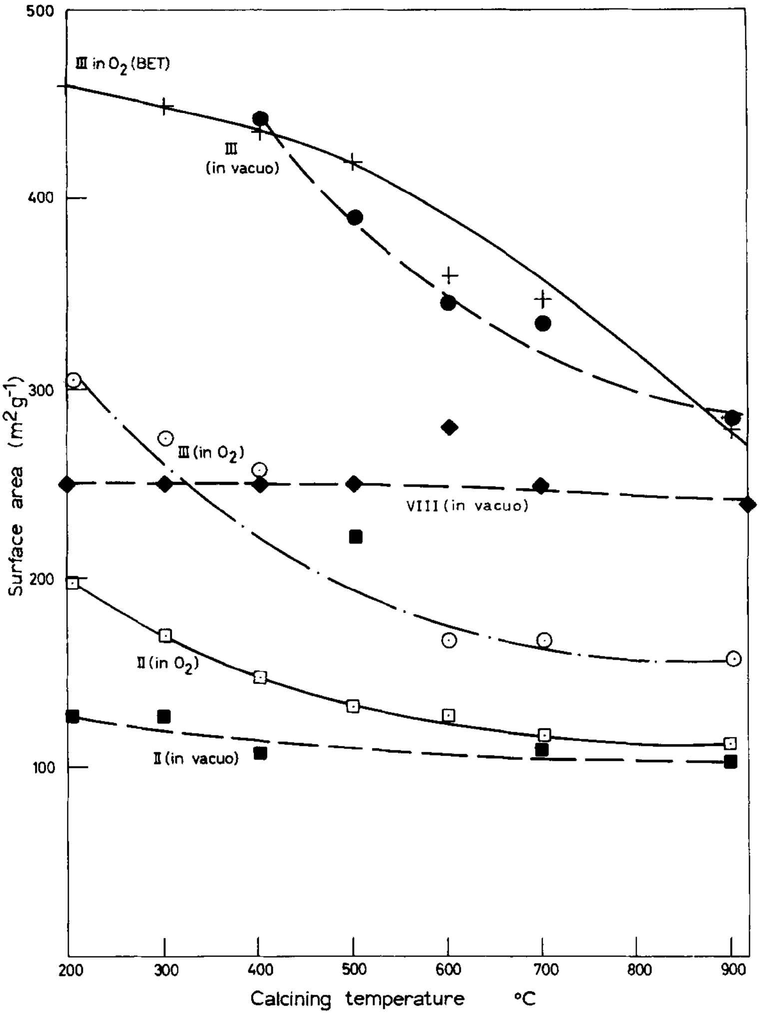

FIG. 5. Variation of external surface areas of alumina aerogels with temperature of preheating. (●) Ether-prepared aerogel heated *in vacuo;* (○) ether-prepared aerogel heated in oxygen; (■) alcohol-prepared aerogel heated *in vacuo;* (□) alcohol-prepared aerogel heated in oxygen; (♦) hexane-prepared aerogel heated *in vacuo;* (+) BET area of ether-prepared aerogel heated in oxygen.

The alcohol-prepared aerogels follow the same tendency as the nitrogen α_s-plots in that there is a steady tendency (with the exception of the 300°C values) for the carbon tetrachloride uptake to fall with increasing temperature and to give curves which become nearly parallel to the α_s-axis at high α_s-values. Micropore volumes, calculated as described for the nitrogen plots, are shown in Table 2 and are seen to be somewhat larger than the corresponding values derived from nitrogen α_s-plots. The anomalous behavior of the 300°C sample may be due to incipient pyrolysis of organic molecules in the pores.

The ether-prepared aerogels behave quite differently. The carbon tetrachloride uptake increases markedly as the calcination temperature is raised, reaching a maximum at 500°C and falling again slightly at 900°C. No leveling off at higher α_s-values was discernible although we were limited experimentally to $\alpha_s < 1.2$ as the microbalance was unable to accommodate the very large increase in weight even at these low α_s-values. This effect could be explained either by the narrowing of relatively large pores into the mesopore range causing the onset of capillary condensation to be brought down to the low range of α_s observed, or, more probably, by the unsealing of pores of restricted opening to give mesopores previously inaccessible to the carbon tetrachloride molecule. In the case of the alcohol-prepared samples, the unsealing does not occur and no upward deviation of the α_s-plots is observed.

Correlation of adsorption data with infrared spectra. The combination of adsorption and electron micrograph data enable us to propose a model which can explain qualitatively why alcohol-prepared aerogels give spectra of trapped carbon dioxide whereas those prepared using other organic liquids do not. We assume that molecules are trapped within a pore when the exit is of the same size, or smaller than, their maximum dimensions. We assume that free rotation is possible, even if the method of mass transport is by 2-dimensional diffusion along the walls of the pore, as proposed by Ash, Baxter and Barrer (*23*).

Electron micrographs give a clear picture of the aerogels as a mass of long, thin needles of alumina, probably fused together at the points of contact to form a 3-dimensional mesh. The pores in the surface texture are the spaces bounded by the needles. It is possible to calculate the external surface area from the average dimensions of the needles by applying the simple relation (*17*):

$$S_{\text{em}} = \frac{4}{\rho d}, \tag{1}$$

where S_{em} is the surface area, ρ the crystal density of γ-alumina and d the diameter of the needles. Values of S_{em} for the alcohol- and ether-prepared aerogels after heating to 600°C in air are 200 and 400 $m^2\ g^{-1}$, respectively, much higher than the corresponding areas derived from the nitrogen α_s-plots for samples heated in oxygen, viz, 128 and 168 $m^2\ g^{-1}$. The discrepancy is probably due to the presence of the large lamellae in the micrographs which add little weighting to the surface area in relation to their relatively large mass.

The mesh structure which the micrographs disclose implies that relatively large pores, in the range 20–200 Å diameter, must be present whereas the infrared results (*1*) show that some at least of these cavities must be sealed by restricted exits of less than 8 Å in order to trap organic molecules and carbon dioxide. The infrared spectra also show that the trapped molecules display a *quasi*-liquid structure, particularly ethanol with its characteristic broad hydrogen-bonded hydroxyl bands. According to Franks and Ives (*24*), liquid alcohols form polymers of a few molecules linked together in a linear fashion. In the present case, this implies that some of these sealed pores are at least 25 Å in diameter to allow this liquid-like association to occur.

The evidence of the electron micrographs and the improved spectra can be reconciled by assuming therefore that although both the alcohol- and the ether-prepared aerogels have the same basic interlocking mesh structure, some of the pores are sealed off with restricted entrances of 8 Å diameter or less. Furthermore, the two types of aerogel differ in some way in that the carbon tetrachloride α_s-plots show that the pores in the ether-prepared aerogels open up on heating whereas those of the alcohol-prepared aerogels do not. This explains why on heating in air or oxygen, when the trapped organic molecules are oxidized by oxygen (σ = 4.2 Å) to carbon dioxide (σ = 5–6 Å), the latter can escape from the ether-prepared aerogel but not from the alcohol-prepared.

The reason for the difference in behavior is not entirely clear but the α_s-plots show that the alcohol-prepared aerogels always have lower external surface areas and smaller narrow pore volumes than the corresponding ether-prepared samples. The electron micrographs confirm this and show that the difference is due to increased sintering of the alcohol-prepared aerogels. It is significant that Vicarini, Nicolaon and Teichner (*25*) found that traces of water promoted the crystallization of titania and zirconia aerogels during the autoclaving process. No special precautions were taken in the present work to exclude traces of water from the materials used during the preparation of aerogels and as ethanol is in any case much more difficult to dry than ether, it is probable that the presence of water, combined with the higher autoclaving temperature used (250°C as against 220°C) has led to the increased sintering of the alcohol-prepared aerogels.

Our observation (*1*) that γ- and χ-aluminas are formed rather than the boehmite expected from such relatively low temperatures, may be explained in terms of an accelerated hydrothermal transition, catalyzed by traces of water. Hexane- or other hydrocarbon-prepared aerogels where water was removed to an even greater extent than for ether and where the critical temperature was even lower (190°C), gave aerogels with the boehmite structure.

The pore structure of the aerogels is stabilized during the autoclaving process. The increased crystallinity of the alcohol-prepared aerogels conferred at this stage probably means that the small openings do not open up on subsequent calcination and therefore the encapsulated carbon dioxide does not escape until the whole pore structure finally collapses to give high density α-alumina. On the other hand, the pore openings in the less well crystallized ether-prepared aerogels, which are initially only slightly larger than those in the alcohol-prepared aerogels, probably open up on heating; this allows carbon dioxide to escape and renders the pores accessible to the carbon tetrachloride adsorbate molecules.

ACKNOWLEDGMENTS

The authors would like to thank the Gas Council for permission to publish these results, which were obtained at the laboratories of the London Research Station.

REFERENCES

1. PARKYNS, N. D., *J. Catal.* **27,** 34 (1972).
2. LIPPENS, B. C., LINSEN, B. G., AND DE BOER, J. H., *J. Catal.* **3,** 32 (1964).
3. LIPPENS, B. C., AND DE BOER, J. H., *J. Catal.* **4,** 319 (1965).
4. DE BOER, J. H., LINSEN, B. G., AND OSINGA, T. J., *J. Catal.* **4,** 643 (1965).
5. BROEKHOFF, J. C. P., AND LINSEN, B. G., *in* "Physical and Chemical Aspects of Adsorbents and Catalysts" (B. G. Linsen, ed.). Academic Press, London, 1970.
6. PIERCE, C., *J. Phys. Chem.* **72,** 3673 (1968).
7. CRANSTON, R. W., AND INKLEY, F. A., *in* "Advances in Catalysis" (W. G. Frankenburg, V. I. Komarewsky, and E. K. Rideal, eds.), Vol. 9, p. 143. Academic Press, New York, 1957.
8. BRUNAUER, S., SKALNY, J., AND BODOR, E. E., *J. Colloid Interface Sci.* **30,** 546 (1969).
9. SING, K. S. W., *in* "Surface Area Determination" (D. H. Everett and R. H. Ottewill, eds.). Butterworths, London, 1970.
10. CUTTING, P. A., *in* "Vacuum Microbalance Techniques" (C. H. Massen and H. J. Van Beckum, eds.), Vol. 7. Plenum, New York, 1970.
11. PAYNE, D. A., AND SING, K. S. W., *Chem. Ind. (London)* 918 (1969).
12. SING, K. S. W., *Chem. Ind. (London)* 829 (1967).
13. CUTTING, P. A., thesis, Brunel Univ., 1970.
14. PERI, J. B., *J. Phys. Chem.* **69,** 211 (1965).
15. SHULL, C. G., *J. Amer. Chem. Soc.* **70,** 1410 (1949).
16. ARISTOV, B. G., AND KISELEV, A. V., *Kolloid. Zh.* **27,** 289 (1965).
17. GREGG, S. J., AND SING, K. S. W., "Adsorption, Surface Area and Porosity." Academic Press, London, 1967.
18. "Tables of Interatomic Distances." Chemical Society, London, 1958.
19. LANDBOLT-BORNSTEIN, "Zahlenwerte und Funktionen." Springer, Berlin, 1962.
20. HEXTER, R. M., AND GOLDFARB, T. D., *J. Inorg. Nucl. Chem.* **4,** 171 (1957).
21. MIKHAIL, R. S. L., BRUNAUER, S., AND BODOR, E. E., *J. Colloid Interface Sci.* **26,** 45 (1968).
22. CARRUTHERS, J. D., PAYNE, D. A., SING, K. S. W., AND STRYKER, L. J., *J. Colloid Interface Sci.* **36,** 205 (1971).
23. ASH, R., BAXTER, R. W., AND BARRER, R. M., *Proc. Roy. Soc., Ser. A.* **299,** 434 (1967).
24. FRANKS, F., AND IVES, D. J. G., *Quart. Rev. Chem. Soc.* **20,** 1 (1966).
25. VICARINI, M. A., NICOLAON, G. A., AND TEICHNER, S. J., *Bull. Soc. Chim. Fr.* **5,** 1651 (1970).